

Hsp60 Chaperonin Acts as Barrier to Pharmacologically Induced Oxidative Stress Mediated Apoptosis in Tumor Cells with Differential Stress Response

Upasana Sarangi^{1,#}, Manish Kumar Singh^{2,#}, Kanugovi Vijaya Vittal Abhijanya¹, Lebaka Prasanna Anjaneya Reddy¹, Badabagni Siva Prasad¹, Vikrant Vinay Pitke¹, Khanderao Paithankar¹ and Amere Subbarao Sreedhar¹

¹CSIR—Centre for Cellular and Molecular Biology, Uppal Road, Hyderabad 500007, Andhra Pradesh, India. ²Centre for Genomics, Jiwaji University, Gandhi Road, Gwalior 474011, Madhya Pradesh, India. #Authors contributed equally. Corresponding author email: assr@ccmb.res.in

Abstract: Mitochondrial functions play a central role in energy metabolism and provide survival fitness to both normal and tumor cells. Mitochondrial chaperonin Hsp60 is involved in both pro- and anti-apoptotic functions, but how Hsp60 senses the mitochondria selective oxidative stress response is unknown. In this study, by using rotenone, an irreversible inhibitor of oxidative phosphorylation against IMR-32 and BC-8 tumor cells containing differential heat shock transcriptional machinery, we studied whether the oxidative stress response is related to Hsp60. The accelerated cytotoxicity in response to rotenone has been correlated with enhanced production of $O_2^{\bullet-}$, H_2O_2 , reactive oxygen species, and Hsp60 translocation from the mitochondria to the cytoplasm. The inability of cells to resist oxidative stress mediated Hsp60 translocation appeared to depend on mitochondrial oxyradical scavenging system and Bax translocation. A delayed oxidative stress response in *hsp60* shRNA-treated cells was found to be due to increased mitochondrial translocation of Hsp60 on shRNA pre-sensitization. Overexpression of Hsp60 failed to protect cells from oxidative stress due to a lack of its mitochondrial retention upon post-rotenone treatment. These results also revealed that Hsp60 mitochondrial localization is indispensable for decreasing $O_2^{\bullet-}$ levels, but not H_2O_2 and ROS levels. However, cycloheximide treatment alone induced Hsp60 translocation, while rotenone combination delayed this translocation. In contrast to oxidative stress, MG132 and 17AAG treatments showed mitochondrial retention of Hsp60; however, MG132 combination either with *hsp60* shRNA or 17AAG induced its translocation. Additionally, overexpression of Huntingtin gene also resulted in Hsp60 mitochondrial accumulation. We suggest that Hsp60 may act as a barrier to pharmacological targeting of mitochondria.

Keywords: Hsp60, mitochondria, rotenone, oxidative stress, tumor cells

Drug Target Insights 2013:7 35–51

doi: [10.4137/DTI.S12513](https://doi.org/10.4137/DTI.S12513)

This article is available from <http://www.la-press.com>.

© the author(s), publisher and licensee Libertas Academica Ltd.

This is an open access article published under the Creative Commons CC-BY-NC 3.0 license.



Introduction

Hsp60 is a major mitochondrial chaperonin and plays a crucial role in the folding and assembly of newly imported proteins.¹ Cytoplasmic Hsp60 has been implicated in cell survival through indistinct cellular mechanisms.² Hsp60 functions were thought to be associated with the mitochondrial proteostasis, until Chandra et al,³ showed its cytoplasmic accumulation during apoptosis activation. Although the role of Hsp60 in cancer cells has not been fully explored, it has been suggested that this chaperonin is a potential antitumor target.^{4,5} Considering its role in several pathological models, it is important to understand its intracellular localization specific functions.

Considering both the bioenergetics and cell-death promoting biochemical mechanisms, mitochondria are implicated in cancer progression as well as in cytotoxicity.^{6,7} The prominent features of cancer cells include enhanced resistance to mitochondrial apoptosis.^{8,9} Chaperones such as Hsp70, Hsp90, and Hsp27 act against cellular oxidative stress by contributing to cell survival.^{10–13} Oxidative stress induces Hsp60 synthesis¹⁴ and protects cells *in vitro*^{15,16} and *in vivo*.^{17,18} Further, the oxidative stress induced Hsp60 oxidation has been correlated with decreased cellular protein oxidation and suggests possible antioxidant functions of Hsp60 in yeast and bacteria.^{19–21} However, studies examining higher eukaryotes to understand the concrete mechanistic details are lacking.

Since Hsp60 secretion increases in response to apoptotic stimuli,²² leading to mitochondrial permeability transition pore opening,²³ Hsp60 is thought to be pro-apoptotic. Nevertheless, mammalian Hsp60 exhibits both anti-apoptotic^{24–26} and pro-apoptotic functions.^{27,28} Given that chaperones are involved in mitochondrial dynamics and in deciding cell fate,²⁹ we aimed to understand the cross-talk between mitochondrial oxidative stress and Hsp60 in response to the inhibition of mitochondrial oxidative phosphorylation (OXPHOS) in tumor cells.

In this study, using rotenone, an irreversible inhibitor of OXPHOS against IMR-32 cells that contain intact inducible heat shock transcriptional machinery³⁰ and BC-8 tumor cells that lack inducible heat shock transcriptional machinery,³¹ we showed that the oxidative stress response is related to Hsp60. We demonstrate that Hsp60 mitochondrial localization

is indispensable for decreases in reactive oxygen species (ROS) levels and cytotoxicity. We also show differential Hsp60 response to proteotoxic stress and oxidative stress, and suggest that Hsp60 acts as a barrier to mitochondrial oxidative stress mediated cell death. In conclusion, we show that Hsp60 acts as a primary response to oxidative stress and its cytoplasmic translocation sensitizes cells to apoptosis. Our findings provide insight into the unconventional roles of Hsp60, which may guide innovative therapeutic strategies to combat cancer.

Materials and Methods

Cell culture and maintenance

Rat histiocytoma, BC-8 is a single clone of spontaneously regressing chemically induced AK-5 tumor developed in the laboratory. Human neuroblastoma, IMR-32 cells were obtained from American Type Cell Culture (ATCC, Manassas, VA, USA). Both cells were grown and maintained in DMEM containing 10% fetal bovine serum albumin in the presence of penicillin (100 U/mL), streptomycin (50 µg/mL), and kanamycin (30 µg/mL) at 37 °C in a humidified incubator with 5% CO₂ supply. For treatments, 1 × 10⁶/mL BC-8 cells in suspension and 0.4 × 10⁶/mL IMR-32 cells grown on cover glasses (22 × 22 mm, Fisher Scientific, Waltham, MA, USA) in a 6-well culture dish (Nunc, Thermo Scientific) were incubated with appropriate drugs in complete medium for the required time periods. Drugs used in the present study included rotenone (1 µM; Sigma-Aldrich, St. Louis, MO, USA), cycloheximide (CHX; 10 µM; Calbiochem, San Diego, CA, USA), 17AAG (2 µM; Invivogen, Carlsbad, CA, USA), MG132 (200 nM; Sigma-Aldrich).

Cell-based assays

Fluorescence activated cell sorting (FACS, FACSCalibur, Becton Dickinson, Franklin Lakes, NJ, USA) analysis was performed by staining cells with propidium iodide (50 µg/mL; Sigma-Aldrich). Intracellular ROS (ROSi) was measured as 2',7'-dichlorofluorescein (DCF) fluorescence using CM-H₂DCFDA (2 µM for BC-8 and 5 µM for IMR-32, Dojindo, Kumamoto, Japan) staining. Change in mitochondrial membrane potential ($\Delta\Psi_m$) was measured by JC-1 (40 nM, Invitrogen, Carlsbad, CA,



USA) staining and analyzed using a MoFlow FACS machine (Becton Dickinson, USA). Each experiment was repeated a minimum three times and the data were analyzed using BD Cell-Quest Pro v5.2 software.

DNA fragmentation assay

Cells fixed in 70% ethanol were incubated in citrate-phosphate buffer, pH 8.0 (192 parts of Na_2PO_4 and 8 parts of citric acid) 1 h at room temperature. Cells were then centrifuged (2655 $\times g$ for 5 min), the supernatant was treated with 3 μL of 0.2% NP40 and 3 μL of RNase (1 mg/mL) at 37 °C for 45 min, followed by proteinase K (1 mg/mL) treatment for another 45 min prior to DNA extraction. The DNA was run on 1% agarose gel at 2 V/cm for 16 h, stained with 0.5 $\mu\text{g}/\text{mL}$ ethidium bromide, and observed using UV transilluminator.

High-performance liquid chromatography (HPLC) detection of superoxide ($\text{O}_2^{\bullet-}$) levels

Cells incubated with 10 μM hydroethidine (HE; Invitrogen) for 20 min were washed and stored at -80 °C until further use. Cells were lysed using 0.2 mL Triton X-100 (0.1%), 100 μL lysate was transferred to another tube containing 100 μL 0.2 M HClO_4 in MeOH and incubated on ice for 1 h. The mixture was centrifuged at 20,000 $\times g$ at 4 °C for 30 min (Model 5417R, Eppendorf, Hamburg, Germany), 100 μL supernatant was transferred to fresh tube containing 100 μL 1 M potassium phosphate buffer, pH 2.6, vortexed for 5 min and subsequently centrifuged for 15 min at 20,000 $\times g$ at 4 °C. The clear supernatant was subjected to HPLC (1200 Series, Agilent Technologies, Santa Clara, CA, USA) analysis using an Agilent C18 column (4.6 \times 250 mm; 5 μm particle size) with a gradient of acetonitrile/water from low (mobile phase A) to high (mobile phase B) concentration of acetonitrile containing 0.1% trifluoroacetic acid (TFA) in UV-visible absorption spectra (excitation: 358 nm; emission: 440 nm). The HE oxidation products 2-OH-E $^+$, E $^+$ and E $^+$ -E $^+$ were obtained from the HPLC analysis. Quantification was performed by comparing integrated peak areas between the obtained and standard solutions under identical chromatographic conditions.

Spectrofluorimetric quantification of hydrogen peroxide

Amplex[®] Red (AR) Hydrogen Peroxide/Peroxidase Assay Kit was purchased from Molecular Probes (Invitrogen). Briefly, 15,000 cells were collected in Krebs-Ringer phosphate (KRP) buffer (145 mM NaCl, 5.7 mM sodium phosphate, 4.86 mM KCl, 0.54 mM CaCl_2 , 1.22 mM MgSO_4 , 5.5 mM glucose, pH 7.4). Next, 100 μL of reaction mixture containing 50 μM Amplex[®] Red, 0.1 U/mL horseradish peroxidase (HRP) was added into wells of a black opaque microplate (Corning-Costar 3915, Corning, NY, USA) and pre-warmed for 10 min at 37 °C. The reaction was initiated by the addition of 50 μL cells in KRP buffer and the absorbance (excitation: 560 nm; emission: 590 nm) was measured in a TECAN infinite 200, multifunctional microplate reader (Tecan, Maennedorf, Austria), and no-HRP control values were normalized with the sample values. Results were analyzed using *i*-control software.

Transfection of plasmid into mammalian cells

Transfection of plasmid DNA into mammalian cells was conducted using lipofectamine LTX plus reagent (Invitrogen). To knockdown Hsp60, 60% confluent cells were transfected with 4 μg piGENETMU6 Rep plasmid carrying Hsp60 shRNA (gift from Dr Renu Wadhwa, Japan). To overexpress Hsp60, 2 μg full length *hsp60* cDNA cloned into pEGFP expression plasmid prepared in-house was used. To induce proteotoxicity, 4 μg Huntingtin (Q86) cloned in pEYFP plasmid (gift from Dr Richard Morimoto, USA) was used. Briefly, the plasmid DNA was added to 100 μL incomplete DMEM medium, mixed with 3 μL of lipofectamine LTX plus reagent, and incubated for 5 min at room temperature. Next, 2 μL lipofectamine plus reagent was added to the mix and further incubated for 30 min at room temperature. The mixture was then added drop-wise to cells containing incomplete medium and incubated. After 4 h incubation at 37 °C in a CO_2 incubator, the medium was replaced with 300 μL complete medium and cells were maintained for 24 h at 37 °C. The transfection efficiency was scored by counting GFP-positive cells under a fluorescence microscope as well as examined for total *hsp60* RNA expression. The shRNA transfected cells



were selected using 2 $\mu\text{g}/\text{mL}$ puromycin, and Hsp60 overexpressing cells and Huntington positive cells were selected using 200 $\mu\text{g}/\text{mL}$ G418. We used control transfection and scrambled transfection for all experiments. The experimental values are taken only after normalizing the values to the lipofectamine/control transfection.

Mitochondria fractionation

Cells (9×10^6) were washed with phosphate-buffered saline (PBS) and resuspended in isotonic buffer A (20 mM mannitol, 7 mM sucrose, 1 mM EGTA, 10 mM HEPES, pH 7.5), supplemented with protease inhibitors (1 mM phenylmethylsulfonyl fluoride (PMSF), 10 $\mu\text{g}/\text{mL}$ leupeptin, 10 $\mu\text{g}/\text{mL}$ pepstatin A, 10 $\mu\text{g}/\text{mL}$ soybean trypsin inhibitor, and 10 $\mu\text{g}/\text{mL}$ aprotinin), and homogenized using Dounce glass homogenizer with 100 strokes holding the homogenizer at a 45° angle. The lysate was centrifuged at 800 rpm for 10 min and the supernatant was collected and re-centrifuged at 15294 xg for 10 min. The pellet containing the mitochondrial fraction was suspended in high concentrations of isotonic buffer (400 mM mannitol, 50 mM Tris-HCl, pH 7.2, 5 mg/mL bovine serum albumin, 10 mM KH_2PO_4) and used for further experiments.

Reverse transcription (RT)-PCR analysis

The total RNA was isolated using TRIZOL (Sigma-Aldrich). The first-strand cDNA was prepared from 1 μg total RNA using Prime Script 1st strand cDNA synthesis kit (Takara Bio Inc., Shiga, Japan). The gene-specific cDNA amplifications were performed using qualitative PCR primers in a dual block PCR machine (DNA Engine; Bio-Rad, Hercules, CA, USA). The primers used included human-specific GAPDH (Accession No NM_002046.3), sense, 5'-ACATCGCTCAGACACCATGGGGAA-3'; antisense, 5'-TGACGGTGCCATGGAATTTGCCA-3'; rat-specific GAPDH (Accession No NG_028301.1), sense, 5'-ACCACAGTCCATGCCATCAC-3'; antisense, 5'-TCCACCACCCTGTTGCTGTA-3'; Hsp60 specific to both human and rat (Accession No NM_010477.4), sense, 5'-AAGGTTGGAAGAAAGGGTGTCA-3'; antisense, 5'-CCTTCAACACAGCTACTCCATC-3'. The primers for producing Hsp60 overexpression plasmids were constructed to contain the *Hind*III restriction site and the antisense primer contained the *Bam*HI

restriction site, (Accession No NM_010477.4), sense, 5'-TGCAGAAGCTTATGCTTCGACTACCCACAG-3'; antisense, 5'-ATTGATGGATCCTTAGAACATGCCGCCTCC-3'.

Immunoblot analysis

Proteins were extracted into HEPES lysis buffer (20 mM HEPES, 10 mM NaCl, 1.5 mM MgCl_2 , 0.1% Triton X-100, pH 7.6), after which 20 μg of the extract was run on 10% SDS-PAGE and transferred to nitrocellulose membrane. The antibodies used in this study included Hsp60 (SPA-806; Enzo Life Sciences, Farmingdale, NY, USA), Bax (Cat No 06-499; Upstate Biotechnologies Inc., Lake Placid, NY, USA), Procaspase-3 (SC-1225), p53 (SC-6243), Bcl2 (SC-783), MnSOD (SC-30080), Cu-Zn SOD (SC-11407), Huntingtin (SC-8767), β -tubulin (SC-9104), COXIV (SC-58348), and GAPDH (SC-25778) were from Santa Cruz, CA, USA. Secondary antibodies used in the study included rabbit anti-goat IgG HRP (SC-2922) and goat antimouse IgG HRP (SC-2005) from Santa Cruz Biotechnology (Santa Cruz, CA, USA). Immunodetection was performed using a Roche chemiluminescence detection kit (Roche, Basel, Switzerland).

Laser scanning confocal imaging microscopy

Mitochondria were stained with CMX-Ros (200 nM; Invitrogen) and the nucleus was stained with DAPI (50 nM; VECTASHIELD, Vector Labs, Burlingame, CA, USA) and observed under a laser scanning confocal imaging microscope (Leica TCS SP5, Leica Microsystems, Solms, Germany). All immunofluorescence experiments were performed using anti-Hsp60 polyclonal primary antibodies and rabbit IgG secondary antibodies conjugated to fluorescein isothiocyanate (FITC) (Santa Cruz Biotechnology).

MTT assay

Control and rotenone-treated cells (1×10^4) in 96-well plates or cells transfected with Hsp60-GFP expression plasmid alone or in combination with rotenone were cultured for 24 and 48 h at standard culture conditions. After treatment, MTT (50 $\mu\text{g}/\text{well}$) was added to the cells and incubated for 4 h. The reaction was stopped by adding 0.1 mL dimethylsulfoxide, and the absorbance of purple color developed was mea-



sured at 570 nm in an enzyme-linked immunosorbent assay plate-reader (Molecular Devices, Sunnyvale, CA, USA). The control values were normalized and the absorbance values obtained were converted to percent cytotoxicity.

Statistical analysis

The data shown are mean \pm standard deviation (SD) or mean \pm standard error of the mean (SEM) of three independent experiments. Significance was calculated by student's *t*-test, data with a value of $P < 0.05$ (*) considered significant.

Results

Rotenone induces cytotoxicity without inducing cytostasis

In this study, by using rotenone, an irreversible inhibitor of oxidative phosphorylation against IMR-32 and BC-8 tumor cells that exhibit differential heat shock transcriptional machinery, we studied whether the oxidative stress response is related to Hsp60. Compromised transcription in BC-8 occurs due to inability of heat shock transcription factor-1 (HSF1) activation. Compromised transcription in BC-8 is due to the lack of heat shock transcription factor-1 activation.³¹ Tumors arise from dysfunctional mitochondria and enhanced Hsp expression; therefore, using two different cells, we examined whether tumor mitochondria play a significant role in deciding the fate of cells as well as the role of Hsp60 chaperonin in its regulation. To study the effect of OXPHOS inhibition in BC-8 and IMR-32, cells were treated with 1 μ M rotenone for 24 and 48 h and analyzed by FACS. DNA content analysis is a standard method to examine cell cycle stages. The cells containing one copy of DNA are grouped as G1 phase cells, cells containing two copies of DNA are grouped as G2/M phase cells, and cells in DNA synthesis phase are grouped as S phase. Cells neither in G1/S nor in G2/M, but with fragmented DNA, a characteristic feature of apoptotic cell death, are grouped as subG1 cells. BC-8 cells showed a time-dependent increase in subG1 cells, 43 and 94% ($P < 0.001$) for 24 and 48 h, respectively with decreased G1 and S phase cells (Fig. 1A). IMR-32 cells also showed an increase in subG1 cells, 29.7 ($P < 0.001$) and 41.75% ($P < 0.01$) for 24 and 48 h, respectively (Fig. 1B). There was a 52% increase in cytotoxicity upon longer treatment of BC-8 compared to IMR-32. Since Hsp60

is implicated in cell death activation during mitochondrial malfunction,²⁵ cells were transiently transfected (60% and 90% efficiency for BC-8 and IMR-32 cells, respectively) with *hsp60* shRNA for 24 and 48 h and analyzed by FACS. The efficiency of shRNA was confirmed by its ability to decrease *hsp60* mRNA (Suppl Fig. 1). In response to shRNA treatment, BC-8 cells showed a rapid increase in subG1 cells, 22 ($P < 0.05$) and 51% ($P < 0.01$) for 24 and 48 h, respectively (Fig. 1C). However, in IMR-32 cells, shRNA treatment resulted in a small increase in subG1 cells, 12% and 15% ($P < 0.05$) for 24 and 48 h, respectively (Fig. 1D). Next, to examine whether shRNA treatment accelerates rotenone-induced cell death, cells after 48 h shRNA transfection were treated with rotenone for 24 and 48 h and analyzed by FACS. BC-8 cells showed 70% subG1 cells by 24 h ($P < 0.01$) and 75% ($P < 0.01$) subG1 cells by 48 h treatment (Fig. 1E). However, IMR-32 cells showed 44% ($P < 0.001$) subG1 cells by 24 h and 46% subG1 cells by 48 h (Fig. 1F). shRNA treatment did not enhance cell death induced by rotenone by 48 h in BC-8 and IMR-32.

Cytoplasmic translocation of Hsp60 correlates with rotenone-induced cytotoxicity in BC-8 cells

To examine whether rotenone treatment effects Hsp60 localization, mitochondria were stained with CMX-Ros followed by cytoimmunofluorescence with FITC-conjugated anti-Hsp60 antibodies. In BC-8, untreated cells showed Hsp60 localizing to mitochondria, but rotenone treatment resulted in a significant decrease in mitochondrial Hsp60 (Fig. 2A, left panel). BC-8 cells showed rapid decrease in mitochondrial Hsp60 compared to IMR-32. In BC-8, the cytoplasmic translocation of Hsp60 is evident at 24 h time intervals; however, at 48 h, due to enhanced cytotoxicity, Hsp60 localization was observed neither in mitochondria nor in cytoplasm (Fig. 2A, left panel). In IMR-32, though a significant decrease in mitochondrial Hsp60 at 24 h was observed, an increase in both cytoplasmic and mitochondrial Hsp60 was observed at 48 h. A complete translocation of Hsp60 in BC-8 also resulted in increased mitochondrial mass and engorgement; in contrast, there was an increase in Hsp60 levels in IMR-32 correlating with intact mitochondria (Fig. 2A, right panel). To further confirm Hsp60 localization, the cytosol

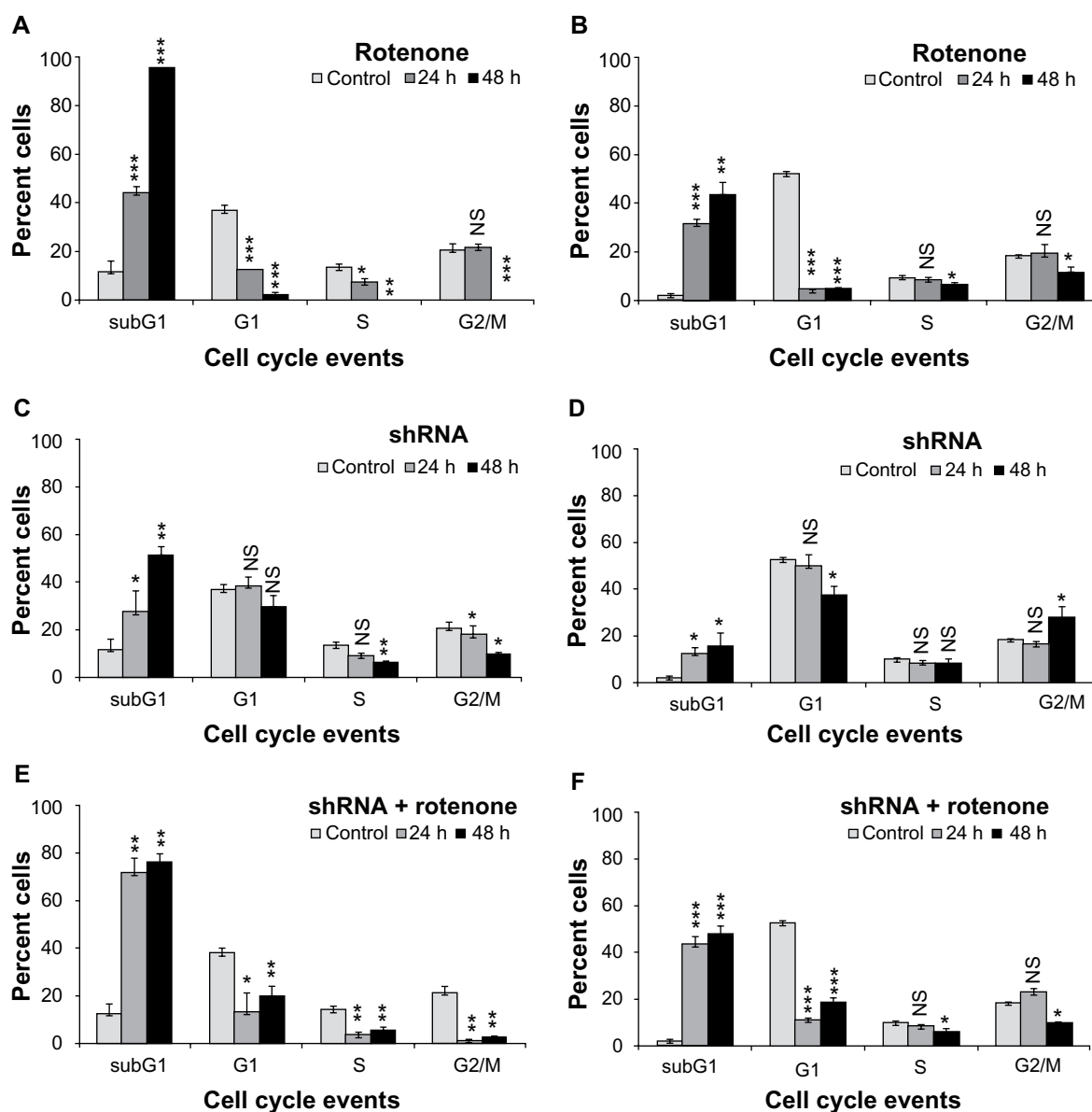


Figure 1. Rotenone induces cytotoxicity independently of cell cycle inhibition. BC-8 cells were treated with (A) rotenone, (C) shRNA, and (E) combination for 24 and 48 h and were analyzed by FACS. IMR-32 cells treated with (B) rotenone, (D) shRNA, and (F) combination for 24 and 48 h were analyzed by FACS. Based on DNA content analysis, cell cycle phases were separated and are represented in the bar diagram. White bars are untreated cells, grey bars are 24 h treatment, and black bars are 48 h treatment. The Y-axis represents percent cells in each cell cycle phase mentioned in the X-axis. The values represented are mean \pm SD. To calculate statistical significance, control values were compared with 24 and 48 h treatments. * $P < 0.05$; ** $P < 0.01$; *** $P < 0.001$; NS, not significant.

and mitochondria fractions were separated purity was confirmed using cytochrome c oxidase (COXIV) analysis in cytosolic fractions. The proteins were run on 10% SDS-PAGE and immunoblotted with antiHsp60 antibodies. The densitometry values after normalizing with mitochondrial protein COXIV were used for plotting the graphs. The results clearly indicated enhanced cytosolic translocation of Hsp60 only in BC-8 (Fig. 2B, left panel), but not in IMR-32 cells (Fig. 2B, right panel).

shRNA treatment delayed cytosolic translocation of Hsp60

To understand whether knockdown of Hsp60 enhances the rotenone response, cells were either treated with shRNA alone for 48 h or further treated with rotenone for 24 and 48 h, and mitochondria were stained with CMX-Ros followed by cytoimmunofluorescence with Hsp60 antibodies. Interestingly, BC-8, upon rotenone treatment, showed a complete loss of Hsp60 (Fig. 2) and shRNA treatment for 48 h

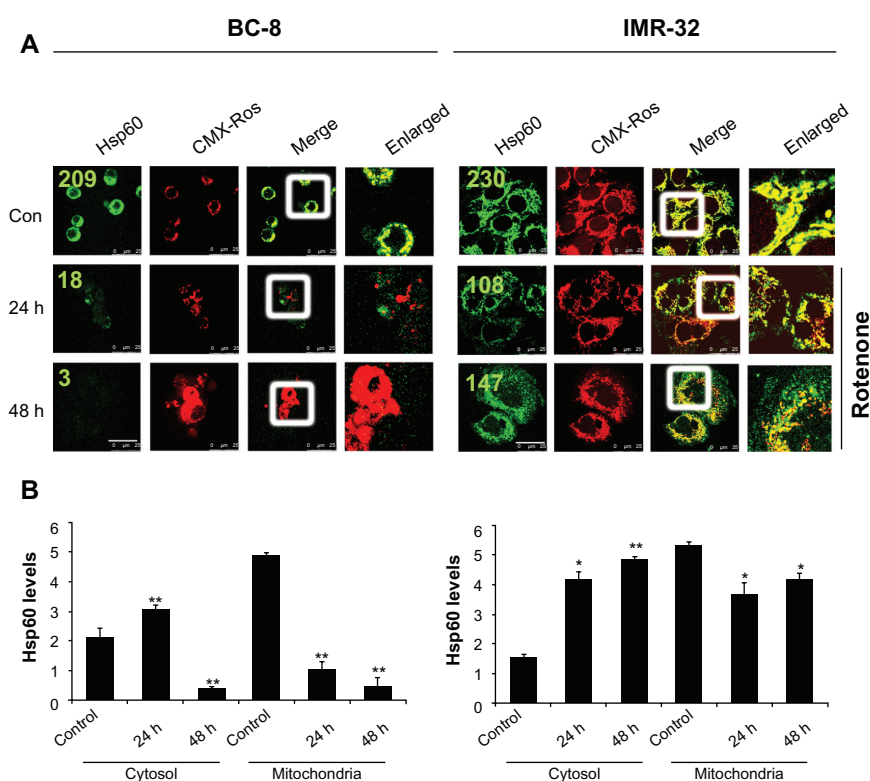


Figure 2. Rotenone promotes the cytoplasmic translocation of mitochondrial Hsp60. **(A)** BC-8 and IMR-32 cells were treated with rotenone, *hsp60* shRNA, or a combination for 24 and 48 h and subjected to cytoimmunofluorescence analysis with anti-Hsp60 antibody (green) and co-stained the mitochondria with CMX-Ros (red). The merger represents the superimposition of green and red images, and the enlarged area indicates the magnified area of the box. Images were captured at 63 \times with a scale bar 25 μ m. **(B)** Statistical representation of cytosol and mitochondria Hsp60 levels from immunoblot analysis and analyzed using ImageJ software. The values represented are from three independent blots. The significance values were calculated from comparison with control from cytosol and mitochondria fractions. The values represented are the mean \pm SD. To calculate statistical significance, control values were compared with 24 and 48 h treatments. * $P < 0.05$; ** $P < 0.01$. The numbers in green indicate fluorescence mean values (ROI).

showed decreased mitochondrial Hsp60. However, a combination of shRNA and rotenone treatment showed complete loss of mitochondrial Hsp60 at this time interval. IMR-32, similar to rotenone treatment (Fig. 1), shRNA alone or in combination with rotenone showed retention of mitochondrial Hsp60 (Fig. 3). Unlike in rotenone treatment in which rapid Hsp60 translocation to cytosol was observed, shRNA treatment showed delayed Hsp60 translocation.

Rotenone-induced ROS production correlates with the cytosolic translocation of Hsp60

Since rotenone induces cytotoxicity through accelerated oxidative stress,³² we measured ROS levels in BC-8 and IMR-32 cells after treating with rotenone, shRNA, or their combination. In BC-8, we observed a time-dependent increase in ROS levels of 56.4 and 96.2% ($P < 0.001$) for 24 and 48 h rotenone treatments, respectively. Although shRNA treatment showed a

small increase in ROS levels, 4.8 ($P < 0.05$) and 19% ($P < 0.01$) for 24 and 48 h, the shRNA combination with rotenone significantly increased ROS levels by 26.93 and 87.33% ($P < 0.01$) for 24 and 48 h, respectively (Fig. 4A). In IMR-32, also we observed a time-dependent increase in ROS levels by 47.1 ($P < 0.01$) and 74.34% ($P < 0.001$) for 24 and 48 h treatments, respectively. Similar to BC-8, shRNA treatment resulted in 1.8 (NS) and 3.9% ($P < 0.01$) increase in ROS levels; however, the shRNA combination with rotenone treatment significantly increased the ROS levels by 70% and 62.6% ($P < 0.001$) for 24 and 48 h treatment, respectively (Fig. 4B). These results suggest that rotenone, but not shRNA treatment, enhances ROS production.

Because the mitochondrial membrane potential provides information regarding mitochondrial damage,³³ cells treated with rotenone, shRNA, and their combination were stained with JC-1 and analyzed by FACS. Under normal physiological conditions,

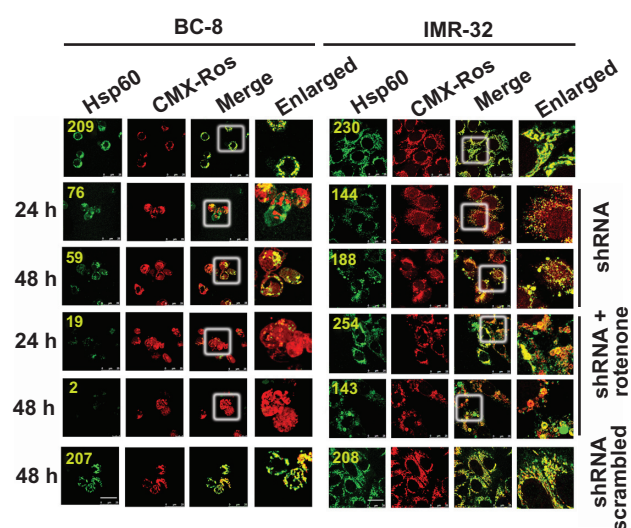


Figure 3. Rotenone combination enforces Hsp60 translocation to cytoplasm despite shRNA induced delay. BC-8 and IMR-32 cells were treated with rotenone, *hsp60* shRNA, or their combination for 24 and 48 h and subjected to cytoimmunofluorescence analysis with anti-Hsp60 antibody (green). Mitochondria stained with CMX-Ros (red). The merger represents the superimposition of green and red images, and the enlarged area indicates the magnified area of the box. Scrambled shRNA was also used and compared with the control. Images were captured at 63 \times with a scale bar 25 μ m. The numbers in green indicate fluorescence mean values (ROI).

JC-1 aggregates in the mitochondria and shows red fluorescence. When the mitochondrial membrane potential collapses, JC-1 cannot accumulate in the mitochondria, and therefore remains in the cytoplasm as a green fluorescent monomeric form. In BC-8, rotenone treatment showed a time-dependent increase in the red to green ratio. However, we did not observe a change in red fluorescence upon shRNA treatment, while rotenone combination treatment significantly increased the red to green ratio (Fig. 4C). In IMR-32 cells, none of the treatments, rotenone, shRNA or their combination, markedly increased green fluorescence (Fig. 4D), suggesting that $\Delta\Psi_m$ may not be directly correlated with ROS production as ROS production is the latter step of superoxide and hydrogen peroxide radical production.

Rotenone induces both superoxide ($O_2^{\bullet-}$) and hydrogen peroxide (H_2O_2) radical production
Complexes I and III of the mitochondrial respiratory chain are the sites for non-enzymatic $O_2^{\bullet-}$ production.³⁴

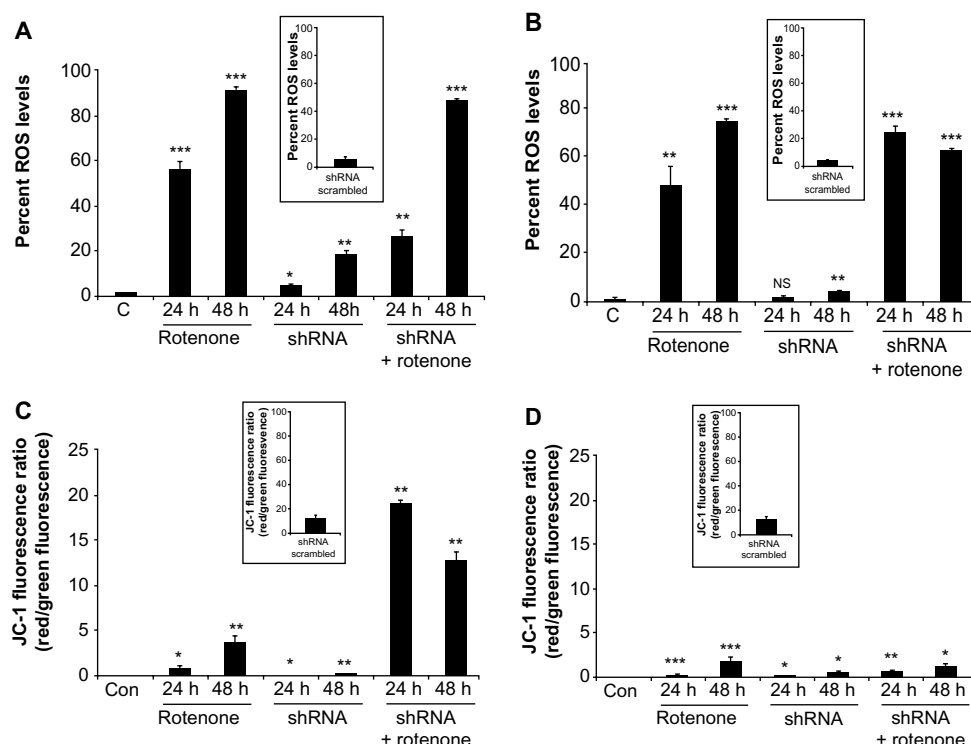


Figure 4. Rotenone, but not *hsp60* shRNA, affects $\Delta\Psi_m$. (A) BC-8 and (B) IMR-32 cells were treated with rotenone, *hsp60* shRNA, and a combination for 24 and 48 h and incubated with H_2DCFDA for 20 min in the dark, then subjected to DCF fluorescence analysis at an excitation wavelength of 488 nm and emission wavelength of 535 nm. C, represents the control. The autofluorescence values were normalized with experimental values and percent DCF fluorescence is represented in the bar diagram. Each bar represents a minimum of five independent experiments. (C) BC-8 and (D) IMR-32 cells after treatment were incubated with JC-1 for 15 min in dark and the red to green JC-1 fluorescence ratio was measured and is represented in the bar diagram. The inset image is shRNA treatment for respective measurements. The values represented are mean \pm SEM. To calculate statistical significance, control values were compared with 24 and 48 h treatments. * $P < 0.05$; ** $P < 0.01$; *** $P < 0.001$.

To examine $O_2^{\bullet-}$ production, oxidation products of hydroxyethidine (HE) were measured by HPLC. In BC-8, rotenone treatment resulted in a significant increase in HE oxidation product 2-OH-E+ (2-hydroxyethidium) both in 24 and 48 h treatments. Following shRNA treatment or shRNA treatment in combination with rotenone, we did not observe the HE oxidation product 2-OH-E+, suggesting inhibited or delayed $O_2^{\bullet-}$ production (Fig. 5), which may be related to Hsp60 retention in the mitochondria (Fig. 3). In IMR-32, in agreement with Figure 1, none of the treatments showed increased $O_2^{\bullet-}$ production (Fig. 5). Although no significant increase in $O_2^{\bullet-}$ production in IMR-32 (Fig. 5) was observed, there was an increase in ROS levels (Fig. 4), suggesting involvement of H_2O_2 . The peroxidase assay revealed that in BC-8, rotenone and shRNA combination with rotenone significantly increased H_2O_2 levels compared to cells treated with shRNA alone (Fig. 6A and E in comparison with 6C, $P < 0.001$). In IMR-32, only rotenone and its

combination with shRNA increased H_2O_2 levels compared to cells treated with shRNA alone (Fig. 6B and F in comparison with 6D, $P < 0.001$). The increased ROS levels, thus, correlate with the increased $O_2^{\bullet-}$ and H_2O_2 production in rotenone treatment in BC-8, but the increase in H_2O_2 production without $O_2^{\bullet-}$ production in IMR-32 suggests activation of alternate systems such as NADP(H) oxidase.³⁵

Cross-talk between pro- and anti-apoptotic molecules

The H_2O_2 generation is a secondary step of dismutation of $O_2^{\bullet-}$. Since two enzymes, manganese superoxide dismutase (MnSOD) and copper/zinc superoxide dismutase (Cu/ZnSOD), are involved in the dismutation reaction,³⁶ we examined whether these two enzyme systems were present in the cytosol and mitochondrial fractions after rotenone treatment. Although we observed an increased synthesis of Cu/ZnSOD in BC-8, its mitochondrial localization was not significant. An inverse response was observed with MnSOD under the same experimental conditions. In IMR-32, a similar but enhanced response was observed (Fig. 7A). These results suggest enhanced MnSOD translocation to the mitochondria may decrease H_2O_2 levels.

If mitochondrial decrease in MnSOD is responsible for increased ROS levels in the mitochondria, it should correlate with increased apoptosis. We observed decreased DNA fragmentation in IMR-32 compared to BC-8 cells (Fig. 7B). The enhanced rate of apoptosis in BC-8 cells was further correlated with a drastic decrease in *hsp60* and *p53* mRNA (Fig. 7C). To identify any potential pro-apoptotic molecules involved in rotenone-induced apoptosis activation, in the absence of Hsp60 synthesis, we examined for potential pro- and anti-apoptotic molecules. Increased mitochondrial Bax correlates with increased apoptosis in BC-8, but not in IMR-32, suggesting that Bax and Hsp60 have opposite functions (Fig. 7D and E).

Rotenone restores cycloheximide (CHX)-induced translocation of Hsp60

To examine whether Hsp60 mitochondrial localization depends on protein synthesis, protein synthesis was inhibited by CHX and Hsp60 localization was observed by cytoimmunofluorescence. Significant translocation of Hsp60 from the mitochondria to the cytoplasm was observed in a time-dependent

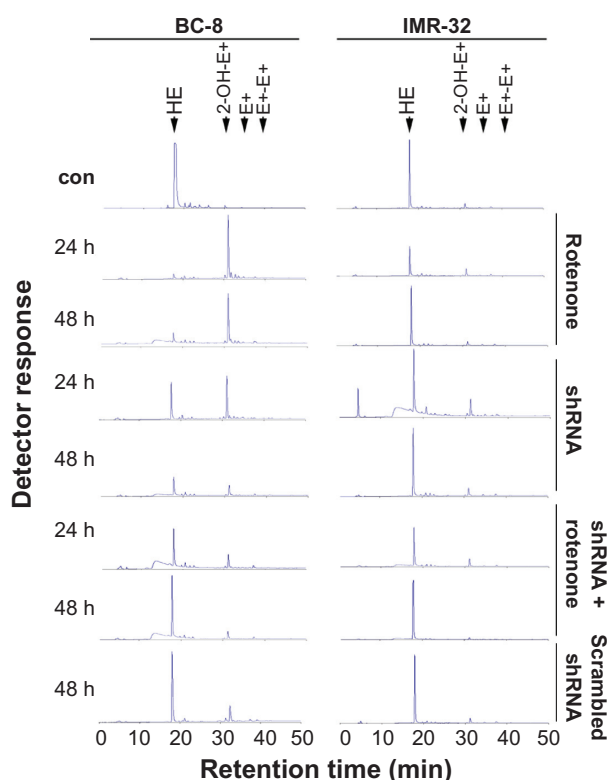


Figure 5. Rotenone treatment, but not shRNA, induces $O_2^{\bullet-}$ production. BC-8 and IMR-32 cells were treated with rotenone, *hsp60* shRNA, or their combination for 24 and 48 h, treated with HE for 20 min in the dark, and analyzed by HPLC. Fluorescence products of HE were measured at an excitation of 358 nm and emission of 440 nm and the spectra are shown in the figure. Scrambled shRNA was also used and compared with control. The experiment was repeated at least ten times and a representative spectrum is shown.

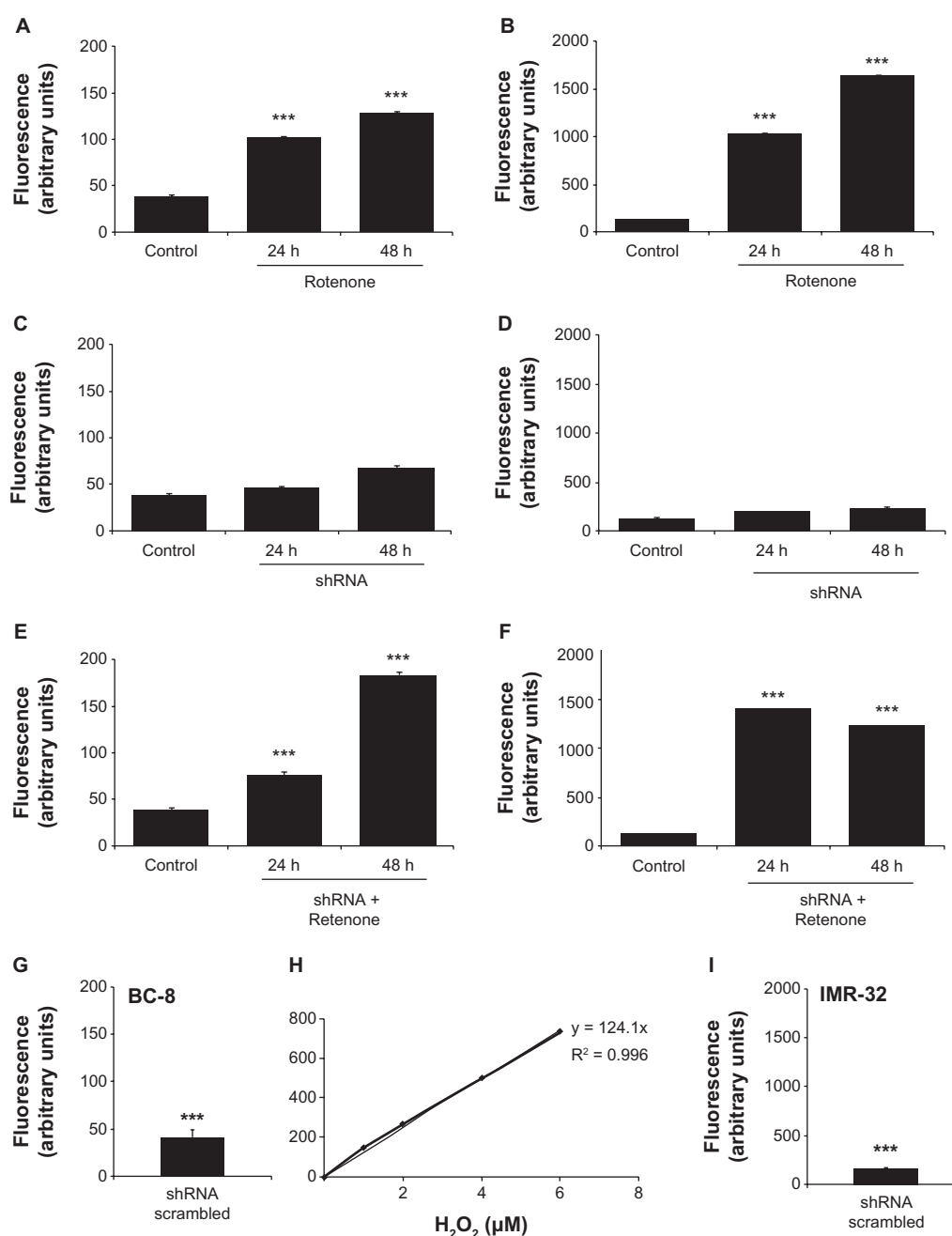


Figure 6. Rotenone treatment, but not *hsp60* shRNA, significantly induces H₂O₂ production. BC-8 cells were treated with (A) rotenone, (C) *hsp60* shRNA, and (E) their combination for 24 and 48 h, treated with AmplexRed for 20 min in the dark, and analyzed. Resorufin excitation and emission were measured at 571 and 585 nm, respectively, in a spectrofluorimeter. Similarly, IMR-32 cells were treated with (B) rotenone, (D) *hsp60* shRNA, and (F) their combination for 24 and 48 h, treated with AmplexRed and analyzed in spectrofluorimeter. (G) Scrambled shRNA treated BC-8 and (I) scrambled shRNA treated IMR-32 cells. (H) Standard curve for H₂O₂ showing the fluorescence response units at the Y-axis and H₂O₂ concentration at the X-axis. The experiment was repeated at least twelve times and average arbitrary values (mean ± SEM) are presented. To calculate statistical significance, control values were compared with 24 and 48 h treatments. ****P* < 0.001.

manner both in BC-8 (Fig. 8A) and in IMR-32 (Fig. 8B) cells. However, CHX combination treatment with rotenone restored mitochondrial Hsp60 at 24 h treatment, but promoted cytoplasmic translocation by 48 h both in BC-8 (Fig. 8A) and in IMR-32 (Fig. 8B) cells.

Exogenous expression of Hsp60 localizes to mitochondria, but rotenone treatment induces its cytoplasmic translocation

BC-8 cells lack inducible transcription of heat shock genes,³¹ however, IMR-32 cells can synthesize Hsps

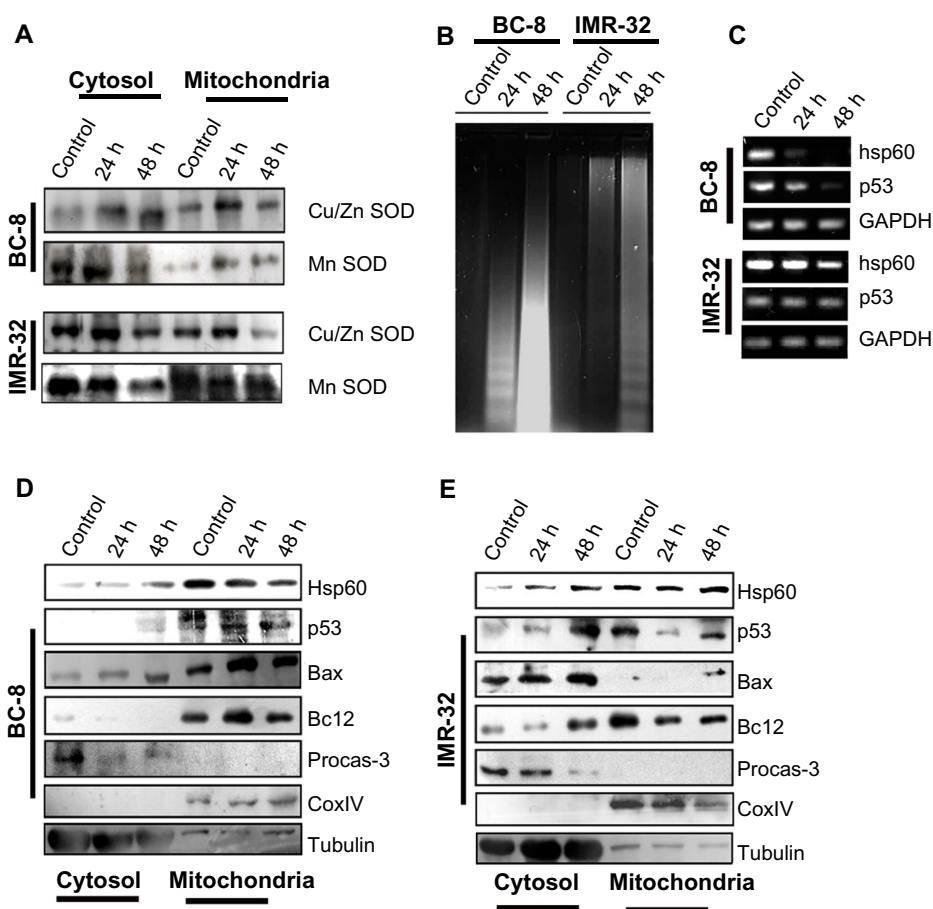


Figure 7. Rotenone alters the expression of pro- and anti-apoptotic regulators. **(A)** Cells were treated with rotenone for 24 and 48 h, cytosol and mitochondria fractions were separated, run on 12% SDS-PAGE, and subjected to immunoblot analysis using anti-cu/ZnSOD and anti-MnSOD antibodies. **(B)** DNA fragmentation analysis of BC-8 and IMR-32 cells after 24 and 48 h rotenone treatments. **(C)** RT-PCR analysis of *hsp60* and *p53* mRNA transcripts. GAPDH was used for loading control. **(D)** Immunoblot analysis of pro- and anti-apoptotic molecules from cytosol and mitochondria fractions of rotenone treated BC-8 cells. The loading controls for BC-8 and IMR32 for Figure 7A are the same in Figure 7D and Figure 7E, respectively. **(E)** Immunoblot analysis of pro- and anti-apoptotic molecules from cytosol and mitochondria fractions of rotenone treated IMR-32 cells. CoxIV is used to show the purity of the mitochondrial fraction and β -tubulin is used to show the purity of the cytosolic fraction.

under stress conditions.²⁹ Therefore, to examine exogenous expression of Hsp60 and whether it is involved in mitoprotection, cells transfected with *hsp60*-GFP plasmid were treated with rotenone and observed for Hsp60 localization. Although exogenously expressed Hsp60 showed mitochondrial localization, rotenone treatment induced its partial cytoplasmic translocation (Fig. 8C). The partial mitochondrial retention decreased $O_2^{\bullet-}$ (Fig. 8D) and H_2O_2 production (Fig. 8E), which correlated with decreased cytotoxicity by 30% ($P < 0.01$) and 20% ($P < 0.001$) for 24 and 48 h, respectively (Fig. 8F).

Hsp60 localizes to the mitochondria upon induced proteotoxicity

To understand the effect of induced proteotoxicity on Hsp60 translocation, IMR-32 cells were treated with

proteasome inhibitor (MG132) and Hsp90 inhibitor (17AAG) and examined for Hsp60 localization. Both MG132 and 17AAG accelerated mitochondrial accumulation of Hsp60 in IMR-32 (Fig. 9A) and BC-8 (Fig. 9B). These results suggest that in contrast to oxidative stress inducers, proteotoxicity inducers retain Hsp60 in the mitochondria. Next, to examine the physiological significance of our findings, IMR-32 cells were transfected with Huntingtin (HTT) mammalian expression system and examined for Hsp60 localization either alone or in combination with *hsp60* shRNA. Huntingtin-transfected cells showed increased Hsp60 mitochondrial localization (compare Fig. 9A with C), whereas shRNA treatment further accelerated its mitochondrial localization (Fig. 9C). These experiments suggest that Hsp60 mitochondrial localization may have mitoprotective roles.

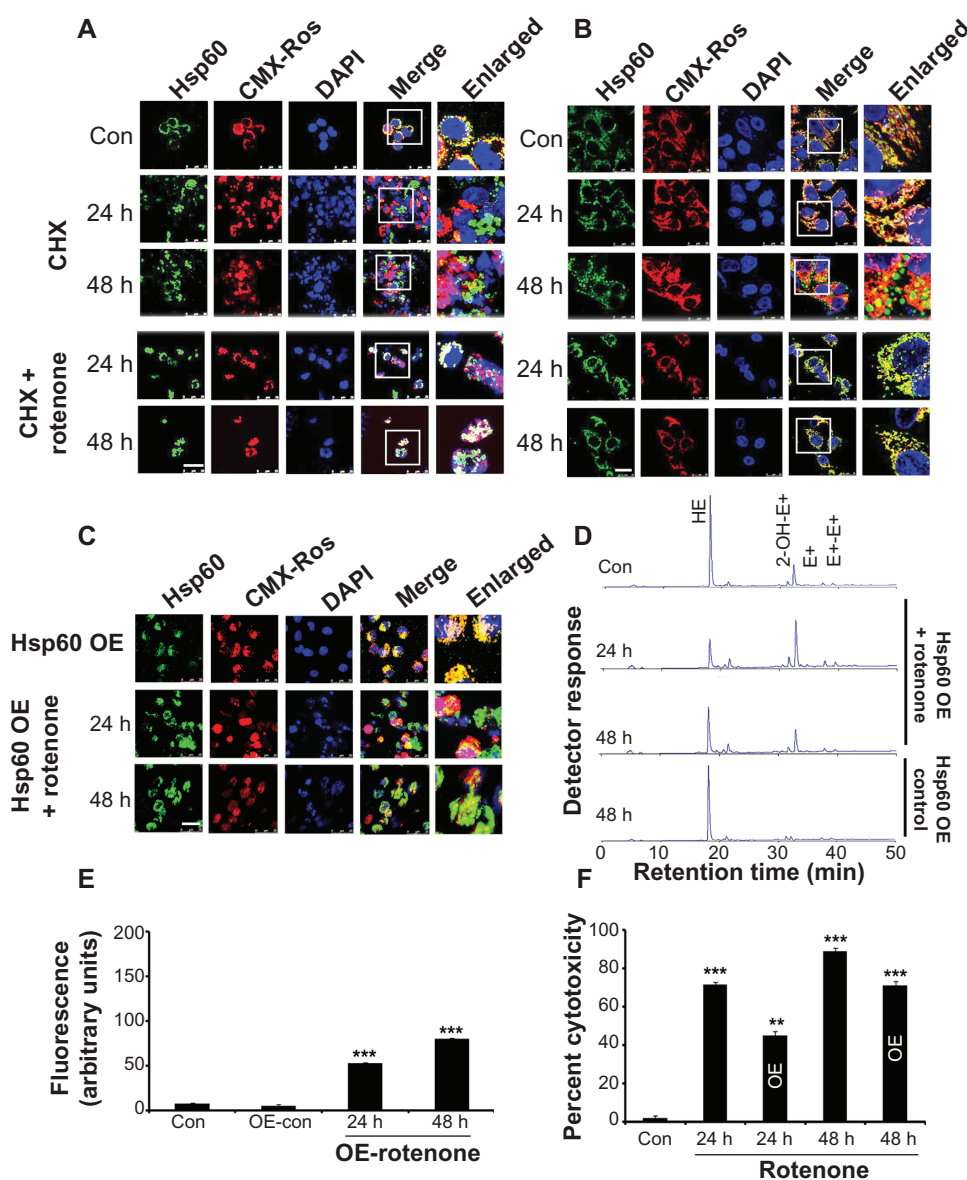


Figure 8. Comparison of cycloheximide with rotenone-induced Hsp60 translocation. (A) BC-8 and (B) IMR-32 cells were either treated with cycloheximide or combined with rotenone for 24 and 48 h were subjected to cytoimmunofluorescence analysis with anti-Hsp60 antibody (green). (C) BC-8 cells transfected with Hsp60 expressing plasmid either alone or combined with rotenone treatment and for 24 and 48 h and analyzed by cytoimmunofluorescence using the anti-Hsp60 antibody. Mitochondria were stained with CMX-Ros (red) and nucleus with DAPI (blue). Images were captured at 63 \times with a scale bar 25 μ m. (D) Analysis of HE oxidation products by HPLC in Hsp60-transfected cells either alone or in combination with rotenone. (E) Analysis of AmplexRed oxidation product, resorufin by spectrofluorimetry in Hsp60 transfected cells, either alone or in combination with rotenone. (F) Cytotoxicity assay of control and rotenone treated cells. Experiments (D–F) were repeated at least twelve times and average arbitrary values (mean \pm SEM) are presented. ** $P < 0.01$; *** $P < 0.001$.

Discussion

Nuclear-encoded chaperones, including Hsp60, play a central role in mitochondrial protein homeostasis.^{37,38} However, whether Hsp60 is pro-survival² or pro-apoptotic³ is controversial. In addition, Hsp60 expression has been linked to tumorigenesis^{2,4,25,39} and cellular transformation.⁴⁰ Thus, we examined the role of Hsp60 against the rotenone-induced mitochondrial oxidative stress response. We demonstrate

that accelerated cytotoxicity in response to rotenone correlates with enhanced production of $O_2^{\bullet-}$, H_2O_2 , ROS, and Hsp60 translocation from the mitochondria into the cytoplasm. We propose that cross-talk occurs between mitochondrial oxidative stress and Hsp60 in response to pharmacological inhibition of OXPHOS in tumor cells.

Considering that complex I of OXPHOS system is the major site for $O_2^{\bullet-}$ production, rotenone

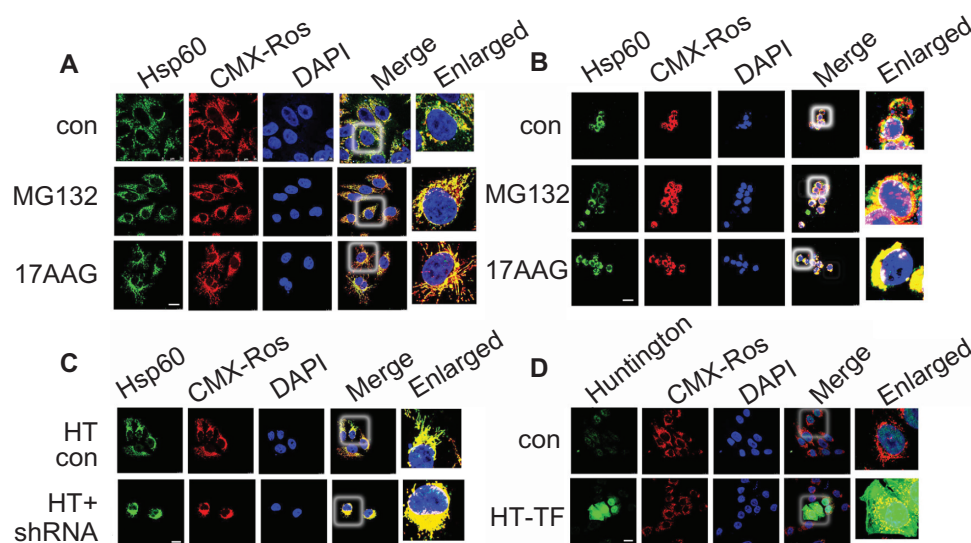


Figure 9. Pharmacologically induced proteotoxicity fails to induce mitochondrial Hsp60 translocation to cytosol. **(A)** IMR-32 and **(B)** BC-8 cells were treated with MG132 or 17AAG and cytoimmunofluorescence was detected with anti-Hsp60 antibody (green). Mitochondria were stained with CMX-Ros (red) and nucleus with DAPI (blue). **(C)** IMR-32 cells were transfected with Huntingtin (Q86) either alone or in combination with *hsp60* shRNA, and cytoimmunofluorescence was detected with anti-Hsp60 antibody. **(D)** IMR-32 cells were transfected with Huntingtin (Q86) and cytoimmunofluorescence analysis was detected with anti-Huntingtin antibody. Images were captured at 63 \times with a scale bar 25 μ m.

is being used in the present study. The rotenone induced polyploidy has specifically correlated with increased $O_2^{\bullet-}$ production, suggesting chromosomal aberrations (Suppl. Fig. 2). Further, the enhanced Hsp60 translocation from the mitochondria to the cytoplasm independent of chromosomal aberrations and cell cycle arrest suggests cell cycle-independent

cell death activation directly mediated by oxidative stress. These findings agree with those of previous reports that rotenone can induce apoptosis as early as 20 min.⁴¹

Despite reports suggesting that ablation of Hsp60 using siRNA can activate the apoptotic response,⁴² we observed no $O_2^{\bullet-}$ production or cytotoxicity with shRNA treatment. However, shRNA in combination with rotenone delayed the cytotoxic response and correlated with increased H_2O_2 and ROS, but not with $O_2^{\bullet-}$ production. The delayed cytotoxicity was later found to be due to Hsp60 retention in the mitochondria in response to shRNA treatment. In contrast to the findings of Isenberg and Klauing,⁴¹ who tested Hsp60 siRNA against normal rat liver cells and showed apoptogenic response mediated by a mitochondrial membrane permeability transition, we observed no significant change in membrane potential either with rotenone or shRNA treatments. Interestingly, following combination treatment, we observed a significant change in membrane potential correlating with H_2O_2 and ROS, but not with $O_2^{\bullet-}$ production. Therefore, the difference in rotenone response may relate to tumor phenotype and their ability to respond to stress and adapt to the tumor microenvironment compared to normal cells.

Subsequent studies showed non-sensitivity of tumor cells to Hsp60 inhibition related to both Hsp60

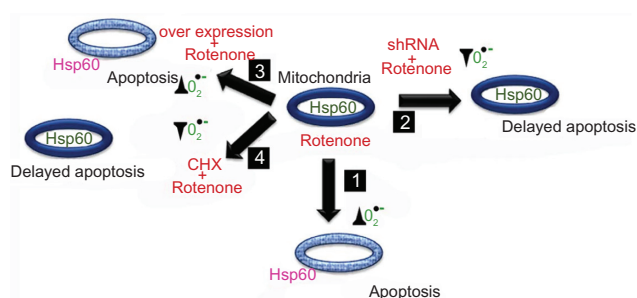


Figure 10. Hsp60 mitochondrion to cytosol translocalization promotes apoptosis and depends on mitochondrion oxidative stress through $O_2^{\bullet-}$ production. Box 1 describes rotenone induced $O_2^{\bullet-}$ production correlating with Hsp60 translocation to the cytosol leading to apoptosis. Box 2 describes delayed $O_2^{\bullet-}$ production, Hsp60 translocation, and apoptosis. Box 3 describes the inability of Hsp60 overexpression to protect cells from rotenone-induced $O_2^{\bullet-}$ production primarily due to the lack of mitochondria localization. Box 4 describes no oxidative stress correlating with mitochondrial Hsp60 and delayed apoptosis. The ovals indicate mitochondria, the thick blue lining of mitochondrion indicates intact mitochondrion, and light blue color indicates altered mitochondrion with altered membrane potential. Hsp60 green color indicates its mitochondrion location and pink color indicates its cytosolic location. The symbol \blacktriangle indicate increases in $O_2^{\bullet-}$ production and \blacktriangledown indicate decreases in $O_2^{\bullet-}$ production.

Abbreviations: shRNA, small hairpin RNA to Hsp60; overexpression, Hsp60 overexpression through transfection; rotenone, rotenone treatments either alone or in combination; CHX, cycloheximide.



abundance and tumor cell tolerance to activate alternate survival mechanisms.²³ In agreement with this, shRNA insensitivity was observed in both tumor cell lines studied.

Further, an enhanced rotenone response was observed in BC-8 with compromised transcription of heat shock genes compared to functionally competent IMR-32 cells. Compromised transcription in BC-8 is due to inability of heat shock transcription factor-1 (HSF1) activation. Further, the enhanced rotenone response was observed in BC-8 that had compromised transcription of heat shock genes compared to functionally competent IMR-32 cells.³⁰ Compromised transcription in BC-8 is due to inability of heat shock transcription factor-1 activation.³¹ Considering that tumor arises due to dysfunctional mitochondria, we used two different cell lines to understand whether tumor mitochondria play any significant role in deciding the fate of cells and, if so, the role of Hsp60 chaperonin in its regulation. Using these two different cell types, we provide new insights on Hsp60 response to rotenone, which can be extended to other mitochondria targeted anticancer agents. To further extend our understanding of Hsp60 functions for chemotherapeutic drugs, we considered its role in oxidative stress tolerance.^{16–19} Our findings confirm the primary response role for Hsp60 in mitochondria mediated oxidative stress sensing, particularly the $O_2^{\bullet-}$ production. The Hsp60 mitochondrial accumulation observed in shRNA treatment appears to be a precautionary measure of cells to protect mitochondria and its cytoplasmic translocation appears to be selective for $O_2^{\bullet-}$ production in response to rotenone treatment.

The rotenone-mediated change in mitochondria organization in IMR-32 cells unlike in BC-8 cells neither correlates with increases in $O_2^{\bullet-}$ production or a change in mitochondrial membrane potential. Further, the dynamics between fusion and fission states is known in mitochondria during normal course of life under normal physiological conditions as well as in response to stress stimulus. Because no harmful outcomes were observed in IMR-32, mitoarchitectural reorganization may be an adaptative response.

Comparison of the effects of shRNA on inhibition of general protein synthesis using cycloheximide provided additional insights. Cycloheximide treatment promoted Hsp60 translocation to the cytoplasm, while its combination with rotenone delayed its cytoplasmic

translocation. The inhibition of protein synthesis compromises mitochondrial functions along with other cellular functions, and may have resulted in severe mitochondrial dysfunction promoting Hsp60 translocation in cycloheximide treatment. Delayed rotenone response in the combination treatment, therefore, may be a result of Hsp60 retention in the mitochondria in early time intervals by some unknown mechanism. Although Shan et al²⁸ suggested that Hsp60 responds independently of cycloheximide, we demonstrated that Hsp60 responds to cycloheximide treatment.

Based on our data, it is clear that mitochondria selective oxidation effects resulted in Hsp60 cytoplasmic translocation. Thus, apoptosis activation occurred through Bax translocation into the mitochondria. Considering the inability of BC-8 cells to synthesize Hsp60, we overexpressed Hsp60 and examined its localization and anti-apoptotic functions. A delay in apoptogenic response to rotenone treatment, but not inhibition, correlated once again with increased $O_2^{\bullet-}$ production, suggesting that endogenous inducible transcription and its mitochondrial retention are necessary for efficient anti-apoptotic functions. Additionally, IMR-32 cells that showed both inducible transcription and efficient retention of Hsp60 in the mitochondria were protected from rotenone-induced cellular insults. The Hsp60 overexpression in BC-8 showed delayed cytotoxicity, but rotenone induced $O_2^{\bullet-}$ production was still able to promote Hsp60 cytoplasmic translocation. In agreement with the observation that Hsps act as anti-apoptotic molecules,^{5,43,44} we demonstrate anti-apoptotic functions for Hsp60 relating to its mitochondrial localization.

Further, to link the proteotoxic stress response with Hsp60 localization in BC-8 and IMR-32 cells, proteotoxicity was promoted either by inhibiting the proteasome functions using MG132 or by inhibiting the major cytosolic chaperone Hsp90 using 17AAG. The accelerated cytoplasmic retention of Hsp60 in response to proteotoxic stress was evident in both cell types, suggesting that accelerated cytoplasmic translocation of Hsp60 occurs only during oxidative stress response. Since both MG132 and 17AAG are pharmacological agents, we extended our study to physiological examples such as overexpression of HTT in IMR-32 cells. Since HTT can directly affect mitochondrial protein traffic, it is expected to induce mitochondria selective proteotoxic stress.⁴⁵ The enhanced accumulation of



mitochondrial Hsp60 further confirmed that proteotoxicity promotes Hsp60 mitochondrial accumulation in contrast to oxidative stress, which promotes its cytoplasmic translocation.

In summary, we show that inhibition of the mitochondrial OXPHOS system using rotenone induces $O_2^{\bullet-}$ production that resulted in DNA damage followed by apoptosis. A time-dependent acceleration in $O_2^{\bullet-}$ production promoted Hsp60 translocation from the mitochondria into the cytosol. Mitochondrial retention of Hsp60 delayed the cytotoxic response and correlated with decreased $O_2^{\bullet-}$ production at the same time intervals. Further, Hsp60 cytoplasmic translocation is specific to the oxidative stress response, but not to proteotoxic stress. We demonstrate how Hsp60 acts as a molecular switch in response to mitochondria specific oxidative stress. Our results establish the mitochondria-specific functions of Hsp60 and indicate that Hsp60 can be used as a pharmacological target for treating cancer.

Abbreviations

Hsp60, heat shock protein 60; OXPHOS, oxidative phosphorylation; $O_2^{\bullet-}$, superoxides; H_2O_2 , hydrogen peroxide; ROS, reactive oxygen species; CHX, cycloheximide; shRNA, small hairpin RNA; $\Delta\Psi_m$, change in mitochondrial membrane potential; SOD, superoxide dismutase; HTT, Huntingtin.

Author Contributions

Performed major experiments discussed in this paper: US, MKS. Performed some of the experiments and acquired the data: KVVA, LPAR, BSP, VVP, KP. Designed the experiments and wrote the manuscript: ASS. All authors reviewed and approved of the final manuscript.

Funding

This work is supported by Council of Scientific and Industrial Research, Government of India.

Competing Interests

Author(s) disclose no potential conflicts of interest.

Disclosures and Ethics

As a requirement of publication the authors have provided signed confirmation of their compliance with ethical and legal obligations including but not limited

to compliance with ICMJE authorship and competing interests guidelines, that the article is neither under consideration for publication nor published elsewhere, of their compliance with legal and ethical guidelines concerning human and animal research participants (if applicable), and that permission has been obtained for reproduction of any copyrighted material. This article was subject to blind, independent, expert peer review. The reviewers reported no competing interests.

References

1. Cheng MY, Hartl FU, Horwich AL. The mitochondrial chaperonin hsp60 is required for its own assembly. *Nature*. 1990;348(6300):455–8.
2. Chun JN, Choi B, Lee KW, et al. Cytosolic Hsp60 is involved in the NF-kappaB-dependent survival of cancer cells via IKK regulation. *PLoS ONE*. 2010;5(3):e9422.
3. Chandra D, Choy G, Tang DG. Cytosolic accumulation of HSP60 during apoptosis with or without apparent mitochondrial release: evidence that its pro-apoptotic or pro-survival functions involve differential interactions with caspase-3. *J Biol Chem*. 2007;282(43):31289–301.
4. Cappello F, Conway de Macario E, Marasà L, Zummo G, Macario AJ. Hsp60 expression, new locations, functions and perspectives for cancer diagnosis and therapy. *Cancer Biol Ther*. 2008;7(6):801–9.
5. Sreedhar AS, Csermely P. Heat shock proteins in the regulation of apoptosis: new strategies in tumor therapy: a comprehensive review. *Pharmacol Ther*. 2004;101(3):227–57.
6. Martinou JC, Youle RJ. Mitochondria in apoptosis: Bcl-2 family members and mitochondrial dynamics. *Dev Cell*. 2011;21(1):91–101.
7. Rohlena J, Dong LF, Neuzil J. Targeting the mitochondrial electron transport chain complexes for the induction of apoptosis and cancer treatment. *Curr Pharm Biotechnol*. 2013;14(3):377–89.
8. Fulda S, Gorman AM, Hori O, Samali A. Cellular stress responses: cell survival and cell death. *Int J Cell Biol*. 2010;2010:1–23.
9. Barja G. Mitochondrial oxygen radical generation and leak: sites of production in states 4 and 3, organ specificity, and relation to aging and longevity. *J Bioenerg Biomembr*. 1999;31(4):347–66.
10. Sreedhar AS, Pardhasaradhi BV, Khar A, Srinivas UK. A cross talk between cellular signalling and cellular redox state during heat-induced apoptosis in a rat histiocytoma. *Free Radic Biol Med*. 2002;32(3):221–7.
11. Madrigal-Matute J, Fernandez-Garcia CE, Gomez-Guerrero C, et al. HSP90 inhibition by 17-DMAG attenuates oxidative stress in experimental atherosclerosis. *Cardiovasc Res*. 2012;95(1):116–23.
12. Arrigo AP, Virost S, Chaufour S, Firdaus W, Kretz-Remy C, Diaz-Latoud C. Hsp27 consolidates intracellular redox homeostasis by upholding glutathione in its reduced form and by decreasing iron intracellular levels. *Antioxid Redox Signal*. 2005;7(3–4):414–22.
13. Kalmar B, Greensmith L. Induction of heat shock proteins for protection against oxidative stress. *Adv Drug Deliv Rev*. 2009;61(4):310–8.
14. Barrett MJ, Alones V, Wang KX, Phan L, Swerdlow RH. Mitochondria-derived oxidative stress induces a heat shock protein response. *J Neurosci Res*. 2004;78(3):420–9.
15. Hollander JM, Lin KM, Scott BT, Dillmann WH. Overexpression of PHGPx and HSP60/10 protects against ischemia/reoxygenation injury. *Free Radic Biol Med*. 2003;35(7):742–51.
16. Lee YH, Govinda B, Kim JC, et al. Oxidativestress resistance through blocking Hsp60 translocation followed by SAPK/JNK inhibition in aged human diploid fibroblasts. *Cell Biochem Funct*. 2009;27(1):35–9.
17. Singh MP, Reddy MM, Mathur N, Saxena DK, Chowdhuri DK. Induction of hsp70, hsp60, hsp83 and hsp26 and oxidative stress markers in benzene, toluene and xylene exposed *Drosophila melanogaster*: role of ROS generation. *Toxicol Appl Pharmacol*. 2009;235(2):226–43.



18. Kaetsu A, Fukushima T, Inoue S, Lim H, Moriyama M. Role of heat shock protein 60 (HSP60) on paraquat intoxication. *J Appl Toxicol*. 2001;21(5):425–30.
19. Cabisco E, Tamarit J, Ros J. Oxidative stress in bacteria and protein damage by reactive oxygen species. *Int Microbiol*. 2000;3(1):3–8.
20. Cabisco E, Belli G, Tamarit J, Echave P, Herrero E, Ros J. Mitochondrial Hsp60, resistance to oxidative stress, and the labile iron pool are closely connected in *Saccharomyces cerevisiae*. *J Biol Chem*. 2002;277(46):44531–8.
21. Uccelletti D, Farina F, Pinton P, et al. The Golgi Ca²⁺-ATPase KIPmr1p function is required for oxidative stress response by controlling the expression of the heat-shock element HSP60 in *Kluyveromyces lactis*. *Mol Biol Cell*. 2005;16(10):4636–47.
22. Merendino AM, Bucchieri F, Campanella C, et al. Hsp60 is actively secreted by human tumor cells. *PLoS ONE*. 2010;5(2):e9247.
23. Ghosh JC, Siegelin MD, Dohi T, Altieri DC. Heat shock protein 60 regulation of the mitochondrial permeability transition pore in tumor cells. *Cancer Res*. 2010;70(22):8988–93.
24. Ghosh JC, Dohi T, Kang BH, Altieri DC. Hsp60 regulation of tumor cell apoptosis. *J Biol Chem*. 2008;283(8):5188–94.
25. Itoh H, Komatsuda A, Ohtani H, et al. Mammalian HSP60 is quickly sorted into the mitochondria under conditions of dehydration. *Eur J Biochem*. 2002;269(23):5931–8.
26. Campanella C, Bucchieri F, Ardizzone NM, et al. Upon oxidative stress, the antiapoptotic Hsp60/procaspase-3 complex persists in mucoepidermoid carcinoma cells. *Eur J Histochem*. 2008;52(4):221–8.
27. Gupta S, Knowlton AA. HSP60, Bax, apoptosis and the heart. *J Cell Mol Med*. 2005;9(1):1–58.
28. Shan YX, Liu TJ, Su HF, Samsamshariat A, Mestrl R, Wang PH. Hsp10 and Hsp60 modulate Bcl-2 family and mitochondria apoptosis signaling induced by doxorubicin in cardiac muscle cells. *J Mol Cell Cardiol*. 2003;35(9):1135–43.
29. Vishal C, Kumar JU, Swamy CVB, et al. Repercussion of mitochondria deformity induced by anti-Hsp90 drug 17 AAG in human tumor cells. *Drug Target Insights*. 2011;5:11–32.
30. Taiyab A, Srinivas UK, Sreedhar AS. 17-(Allylamino)-17-demethoxygeldanamycin combination with diferuloylmethane selectively targets mitogen kinase pathway in a human neuroblastoma cell line. *J Cancer Ther*. 2010;1:197–204.
31. Sreedhar AS, Pardhasaradhi BV, Begum Z, Khar A, Srinivas UK. Lack of heat shock response triggers programmed cell death in a rat histiocytic cell line. *FEBS Lett*. 1999;456(2):339–42.
32. Li N, Ragheb K, Lawler G, et al. Mitochondrial complex I inhibitor rotenone induces apoptosis through enhancing mitochondrial reactive oxygen species production. *J Biol Chem*. 2003;278(10):8516–25.
33. Vayssier-Taussat M, Kreps SE, Adrie C, Dall'Ava J, Christiani D, Polla BS. Mitochondrial membrane potential: a novel biomarker of oxidative environmental stress. *Environ Health Perspect*. 2002;110(3):301–5.
34. Turrens JF. Superoxide production by the mitochondrial respiratory chain. *Biosci Rep*. 1997;17(1):3–8.
35. Infanger DW, Sharma RV, Davisson RL. NADPH oxidases of the brain: distribution, regulation, and function. *Antioxid Redox Signal*. 2006;8(9–10):1583–96.
36. Suski JM, Lebiezinska M, Bonora M, Pinton P, Duszynski J, Wieckowski MR. Relation between mitochondrial membrane potential and ROS formation. *Methods Mol Biol*. 2012;810:183–205.
37. Voos W, Röttgers K. Molecular chaperones as essential mediators of mitochondrial biogenesis. *Biochim Biophys Acta*. 2002;1592(1):51–62.
38. Bie AS, Palmfeldt J, Hansen J, et al. A cell model to study different degrees of Hsp60 deficiency in HEK293 cells. *Cell Stress Chaperones*. 2011;16(6):633–40.
39. Ban HS, Shimizu K, Minegishi H, Nakamura H. Identification of HSP60 as a primary target of o-carboranylphenoxyacetanilide, an HIF-1alpha inhibitor. *J Am Chem Soc*. 2010;132(34):11870–1.
40. Tsai YP, Teng SC, Wu KJ. Direct regulation of HSP60 expression by c-MYC induces transformation. *FEBS Lett*. 2008;582(29):4083–8.
41. Isenberg JS, Klaunig JE. Role of the mitochondrial membrane permeability transition (MPT) in rotenone-induced apoptosis in liver cells. *Toxicol Sci*. 2000;53(2):340–51.
42. Li YY, Lu S, Li K, et al. Down-regulation of HSP60 expression by RNAi increases lipopolysaccharide- and cerulein-induced damages on isolated rat pancreatic tissues. *Cell Stress Chaperones*. 2010;15(6):965–75.
43. Samali A, Cotter TG. Heat shock proteins increase resistance to apoptosis. *Exp Cell Res*. 1996;223(1):163–70.
44. Beere HM. “The stress of dying”: the role of heat shock proteins in the regulation of apoptosis. *J Cell Sci*. 2004;117(Pt 13):2641–51.
45. Orr AL, Li S, Wang CE, et al. N-terminal mutant huntingtin associates with mitochondria and impairs mitochondrial trafficking. *J Neurosci*. 2008;28(11):2783–92.

Supplementary Figures

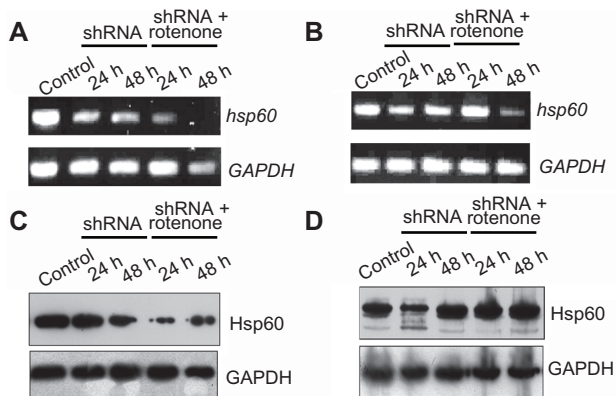


Figure S1. RT-PCR and immunoblot analysis of tumor cells treated with *hsp60* shRNA and shRNA combination with rotenone. (A) BC-8 and (B) IMR-32 cells after treatment with shRNA for 24 and 48 h or followed by rotenone treatment for subsequent time intervals; 24 and 48 h samples were examined for *hsp60* and *p53* expression. *GAPDH* was used to ensure equal cDNA loading. (C) BC-8 and (D) IMR-32 cells showing total Hsp60 protein.

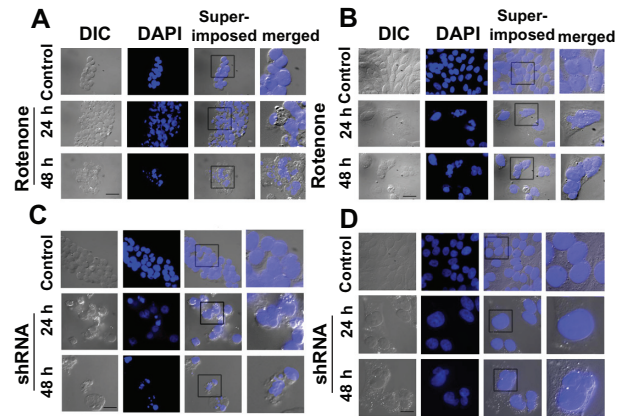


Figure S2. Rotenone treatment, but not shRNA treatment induces polyploidy. (A) BC-8 and (B) IMR-32 cells were treated with rotenone, or (C) BC-8 and IMR-32 cells transfected with *hsp60* shRNA for 24 and 48 h were DAPI stained, cell morphology and nuclear staining was examined under the microscope, DIC and DAPI superimposed images were magnified and represented. Images captured at 63x with a scale bar 25 μ m.